JOURNAL OF SOLID STATE CHEMISTRY **104**, 209–214 (1993)

The Crystal Structure of the Cesium Molybdenum Bronze $Cs_{0.14}MoO_3$

LAURA E. DEPERO AND MARCELLO ZOCCHI

Dipartimento di Ingegneria Meccanica dell'Università, Via Branze,
25123 Brescia, Italy

FERNANDO ZOCCHI

IMAI-CNR Area della Ricerca di Roma, 00016 Monterotondo Stazione, Rome, Italy

AND FRANCESCO DEMARTIN

Istituto di Chimica Strutturistica Inorganica dell'Università degli Studi,
Via G. Venezian 21, 20133, Milan, Italy

Received July 13, 1992; in revised form September 25, 1992; accepted October 2, 1992

The crystal of the title compound is hexagonal, space group $P6_3/m$, with $a = 10.620(9)$, $c = 3.722(2)$ Å, and $Z = 6$. Couples of MoO_6 distorted octahedra, linked by edges, constitute, by repetitive edge sharing along the c axis, ribbons kept together in bundles by lateral corner sharing. These bundles, by being packed together, generate tunnels where delocalized Cs atoms are inserted. The results confirmed the previously found correlation between the Mo oxidation state and the distortion of the coordination "octahedra" and allow one to extend the correlation to the possible conduction properties of the title compound and to those of structurally related oxides and bronzes. © 1993 Academic Press, Inc.

Introduction

It is well known that in most molybdenum oxides (and bronzes) the oxygen coordination polyhedra are more or less distorted octahedra and tetrahedra linked to each other by corner and edge sharing (*1–3*).

In our previous paper (*4*) on the crystal structure of bronze $Cs(Mo_{0.95}W_{0.05})_7O_{21}$ (I) we found a correlation between v, the oxidation state of the Mo atoms in that structure, and ξ, the mean square root deviation of the Mo–O bond lengths, indicating the distortion of the corresponding coordination octahedra. The physical meaning of that correlation is identified by the fact that extra electrons from the alkali metal may occupy the π^* (Mo $d(t_{2g})$—O $p\pi$) antibonding orbitals, thus destabilizing the Mo–O double bonds, increasing the corresponding bond lengths, and reducing the distortions of the coordination "octahedra," while decreasing the value of v.

The present study was prompted by the observation that the title compound, although having a composition very close to that of I and having been prepared following the same chemical route (see below), had a powder diffraction pattern quite different from that of I.

Experimental

Two molybdenum bronzes with approximately the same Cs content have been recently prepared by us: $Cs(Mo_{0.95}W_{0.05})_7O_{21}$ (I) and $Cs_{0.14}MoO_3$ (II), the object of the present work.

According to the method of Ref. (*5*), the reaction leading to the generic cesium molybdenum bronze, Cs_xMoO_3, is

0022-4596/93 $5.00

$$x\mathrm{CsCl} + (x/2)\,\mathrm{WO_2} + \mathrm{MoO_3} \rightarrow \mathrm{Cs}_x\mathrm{MoO_3} + (x/2)\,\mathrm{WO_2Cl_2}.$$

WO_2 is used as a reactant which limits the coefficient x in the bronze, while CsCl is used in excess (typically 30% to 50% in excess).

In the case of I, the amount of WO_2 used was that necessary for obtaining a compound with $x = 0.25$. However, a not-well-defined Mo ⇔ W exchange reaction occurred and the obtained bronze shows a smaller x-value, i.e., exactly $x = 1/7$.

In the present work a mixture of MoO_3, CsCl (in excess), and WO_2, in the amount necessary for obtaining $x = 0.14$, was heated in a silica vial in a vacuum (10^{-4} mbar) at 560°C for 6 days. The product, a mixture of little dark blue crystals of bronze II and white CsCl crystals was washed several times with water to remove CsCl and then dried. No tungsten was observed in the bronze by electron microprobe. In order to determine the value of x, an accurately weighted sample of bronze (about 0.13 g) was melted with a mixture of 0.5 g 99.999% Alfa Ventron KNO_3 and 0.5 g 99.9999% Alfa Ventron K_2CO_3. Then, after cooling, the solidified mass was dissolved in water and the resulting solution analysed by using atomic absorption spectroscopy. The Cs content was found to correspond to $x = 0.14$.

The diffraction experiment was carried out on an Enraf–Nonius CAD4 diffractometer at room temperature, using graphite-monochromated Mo$K\alpha$ radiation ($\lambda = 0.71073$ Å). The intensities of 243 independent reflections, obtained by averaging over the measured 742 intensities ($I > 3\sigma$), were corrected for Lorentz, polarization, and absorption ($\mu = 82.86\ \mathrm{cm}^{-1}$, empirical correction) (*6*) and for extinction ($g = 2.34 \times 10^{-7}$). Scattering factors for all the atomic species and anomalous dispersions corrections for scattering factors of nonhydrogen atoms were taken from Ref. (*7*). The structure was refined by full-matrix least squares. All the calculations were performed on a PDP11/73 computer using the SPD-Plus Structure Determination Package (*8*).

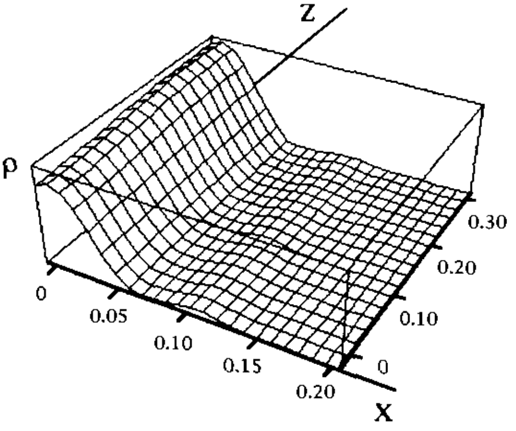

FIG. 1. Fourier difference map with F calculated on the basis of the Mo and O atoms only. Section at $y = 0$. Electron density ρ is given as a function of x and z. The continuous distribution clearly shows cylindrical symmetry with respect to the z axis.

The structure, with the exception of the cesium atom, was solved by direct and Fourier methods and refined by least squares, using an anisotropic model for the thermal motion.

Results

The crystal is hexagonal (space group $P6_3/m$), with $a = 10.620(9)$, $c = 3.722(2)$ Å, and $Z = 6$ for the formula unit $Cs_{0.14}MoO_3$. The a and c parameters were refined using as observations the 2θ positions of 25 Bragg reflections measured on the diffractometer. However they were originally determined by taking long-exposure zero- and first-layer precession photographs of three different crystals. No extra spots or incommensurate reflections were detected and no evidence of a superlattice or of a modulated structure was found.

The cesium atom clearly appeared delocalized in a Fourier difference map, whose coefficients were calculated on the basis of a model containing only Mo and O atoms and with the electron density showing cylindrical symmetry about the **c** axis (Fig. 1).

No convergence was obtained by refining this model based only on those two atomic species. In order to refine the structure by least squares, we derived two models in terms of a "localized" Cs atom, since the Fourier difference map showed that the continuous electron density distribution along the **c** axis had, in fact, two very broad and ill-defined maxima, the larger one (20 electrons/Å^3) at (0, 0, $\frac{1}{4}$) (Wyckoff position 2a) and the smaller one (18 electrons/Å^3) at (0, 0, 0) (Wyckoff position 2b).

While the procedure of refining these "localized cesium models" was performed with the aim of improving the precision of the location of the Mo and O atoms, one should keep in mind that, for both models, the refinement of the Cs atomic and thermal parameters (especially $B(3, 3)$) is only a useful artifact and that here the reality is given by the Fourier difference map showing the continuous electron distribution due to the "delocalized" cesium atom. Thus, within the stated meanings and limitations, two models containing a "localized" Cs atom were refined according to the indications of the Fourier difference map. In Model A the Cs atom was located at (0, 0, $\frac{1}{4}$), while in Model B it was set at (0, 0, 0). In both models an occupancy parameter for Cs was refined from a starting value of 0.07, corresponding to $x = 0.14$. A third model with the Cs atom distributed between the two sites did not converge, showing very heavy correlations between thermal and occupancy parameters. The final values of the conventional R factor are about the same (0.047 and 0.045) for the two models, while, more important, the "error of fit," the estimated standard deviation of an observation of unit weight, is 2.3 and 3.1 for A and B respectively. These values for the error of fit clearly indicate Model A as the "best model," in the sense that it better represents the reality shown by the Fourier difference map. It is interesting to note that the Cesium $\beta(33)$ parameter failed to refine in Model B (its value was kept fixed at a value of 1.5 in the last least-squares cycles), while it converged to a high value of 0.8 in A. In this connection one should also note that in Model A the Cs coordination number (C.N.) is 9, while in Model B the C.N. has a less probable value of 6. For model A the atomic fractional coordinates and the isotropic equivalent thermal parameters B are given in Table I and the anisotropic temperature factors in Table II. Here and in what follows, for the meaning of the term "delocalized" and for the definition of the "localized Model A," one should keep in mind the above considerations and the parameters in Table I. In Model A the Cs occupancy refined from the starting value of 0.070 to 0.065(1), which obviously correlates with the high value of B_{iso} (= 16 Å^2), meaning that the true value of the occupancy of site (0, 0, $\frac{1}{4}$) is probably smaller.

A list of the observed and calculated structure factors for Model A has been submitted as supplementary material.

Discussion

A projection of the structure along the c axis shows a close similarity with that of the well-known hexagonal tungsten bronzes. However, the linkage of the MoO_6 units of approximate octahedral geometry is quite different here (see Fig. 2). Couples of MoO_6 "octahedra," related to each other by inversion centers and linked by edges, constitute,

TABLE I

POSITIONAL AND ISOTROPIC EQUIVALENT THERMAL PARAMETERS (WITH ESTIMATED STANDARD DEVIATIONS)

Atom	x	y	z	B(Å^2)
Cs	0	0	0.25	16(2)
Mo	0.64480(9)	0.10547(9)	0.75	0.30(1)
O(1)	0.5004(7)	−0.2175(7)	0.25	0.7(1)
O(2)	0.4198(8)	−0.0789(7)	0.75	0.5(1)
O(3)	0.7339(8)	0.0110(8)	0.75	0.7(1)

Note. The refined Cs occupancy parameter is 0.065(1). Anisotropically refined atoms are given in the form of the isotropic equivalent thermal parameter.

TABLE II

ANISOTROPIC TEMPERATURE FACTORS (IN Å^2)

Atom	$B(1, 1)$	$B(2, 2)$	$B(3, 3)$	$B(1, 2)$	$B(1, 3)$	$B(2, 3)$
Cs	1.10(6)	B(1, 1)	44(6)	$-B(1, 1)/2$	0	0
Mo	0.22(1)	B(1, 1)	0.21(5)	$-B(1, 1)/2$	0	0
O(1)	0.3(1)	B(1, 1)	1.3(3)	$-B(1, 1)/2$	0	0
O(2)	0.2(1)	B(1, 1)	1.0(3)	$-B(1, 1)/2$	0	0
O(3)	0.2(1)	B(1, 1)	1.6(4)	$-B(1, 1)/2$	0	0

by repetitive edge sharing along the c-axis, ribbons kept together in bundles by lateral corner sharing. Within the ribbons the coordinating Mo atoms form chains of *trans* conformation with Mo–Mo distances of 3.324(1) Å. The bundles, by packing together, generate tunnels where the delocalized Cs atoms are inserted, so that a continuous electron density distribution is present in them. In Model A nine oxygen atoms are coordinated by a Cs atom, three at $z = \frac{1}{4}$ ($R_i = 2.886(5)$ Å), three at $z = \frac{3}{4}$, and three at $z = -\frac{1}{4}$ ($R_i = 3.434(5)$ Å). The oxidation number v of Cs is 1.21, which can be compared with the corresponding value of 1.15 (C.N. = 10) found in I and with that of 1.08 which can be calculated for the cesium molybdate $Cs_2Mo_7O_{22}$ (*9*). While the discrepancy from the expected value of 1 may in part be due to the semiquantitative nature of the parameters R_0 and N used in Brown's formula $s = (R/R_0)^{-N}$, where $R_0 = 1.882$ Å and $N = 6$, it may also reflect the "uneasiness" suffered by the Cs atoms in Model A where the position (0, 0, $\frac{1}{4}$) has three O neighbors at a distance of only 2.886 Å (see above). This "uneasiness" may well be the cause of the observed delocalization of Cs in the structure.

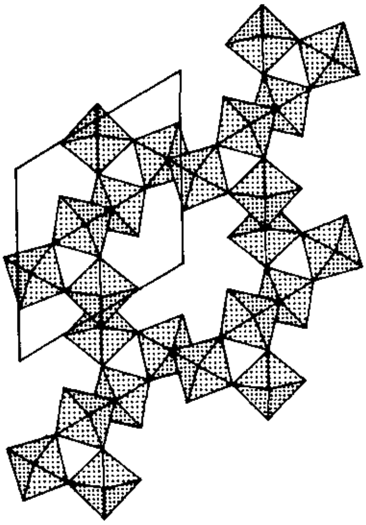

FIG. 2. A view of the structure along the c axis, showing both corner and edge sharing of the distorted Mo-coordination octahedra. The Cs atoms are "delocalized" inside tunnels of hexagonal symmetry.

The Mo–Mo and Mo–O crystallographically independent distances are given, for Model A, in Table III, together with the relevant values of the corresponding bond strengths calculated on the basis of Brown's formula (*10*). In the crystallographically independent "octahedron" two Mo–O distances are very large (>2.2 Å) and, in fact, the coordination geometry can also be described by a tetrahedron. In Fig. 3 a couple of edge sharing "octahedra" are shown with the outlines of the corresponding tetrahedra.

Bond strength calculations (*10*) give for the oxidation number, v, of the Mo atom the value reported in Table III. These results confirm the previously found (*4*) correlation between the valency state v and ξ, the mean square-root deviation, assumed as an index of distortion of the coordination polyhedra. In fact in II there is an additional cause of distortion, this being the relative shift, determined by repulsion, of the two Mo atoms

TABLE III

MODEL A: Mo–Mo AND Mo–O INTERATOMIC DISTANCES (R IN Å) AND Mo–O BOND STRENGTHS (s)[a]

		R	s	
Mo–Mo′	(repeat distance along the c axis)	3.722(2)		
Mo–Mo″	(through edge sharing)	3.324(1)		
Mo–Mo‴	(through corner sharing in the ab plane)	4.005(2)		
Mo–O(1)		2.372(6)	0.249	
Mo–O(1′)		1.707(5)	1.796	
Mo–O(2)		2.205(6)	0.388	
Mo–O(2′)	× 2	1.955(2)	1.592	(0.786 × 2)
Mo–O(3)		1.689(6)	1.894	
$(\text{Mo–O})_{\text{Av}} = 1.981$				
$\xi = 0.270$		$v = \Sigma s_i =$	5.92	

[a] $s = (R/R_0)^{-N}$, $R_0 = 1.882$, $N = 6$ (*10*).

belonging to adjacent edge-sharing "octahedra" (Fig. 3). Indeed the crystallographically independent "octahedron" in II is significantly more distorted than the five independent "octahedra" in I. In Fig. 4 the distortion values ξ vs. the oxidation number v are reported for the mentioned "octahedra" of I and II as well as for those of $\gamma\text{-}Mo_4O_{11}$ (*11*) and those of the K– and Rb–Mo blue bronzes (*12, 13*). It may be interesting to note that, in the figure, points a, d, and h, corresponding to "octahedra" directly linked to tetrahedra by corners are

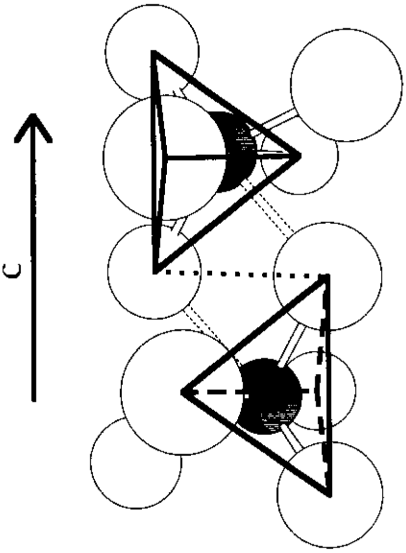

FIG. 3. Two edge-sharing "octahedra" with the outlines of the corresponding tetrahedra of the shortest Mo–O distances.

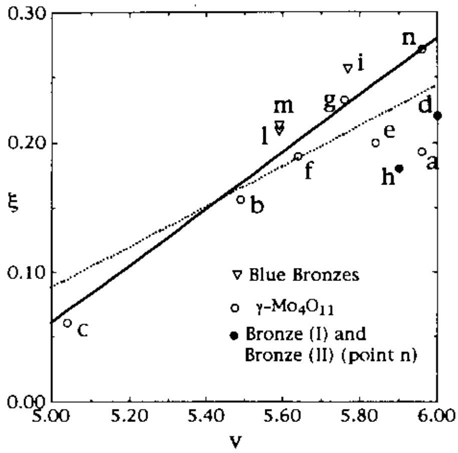

FIG. 4. Distortion values ξ (see text) vs Mo oxidation number v for coordination octahedra in $\gamma\text{-}Mo_4O_{11}$ [11] (points a, b, c), in I (points d, e, f, g, h), and in K– and Rb–Mo blue bronzes (*13*) (points i, l, m). The point corresponding to the Mo octahedron of the title compound is indicated by the letter *n*. The coefficient of correlation $R = 0.931$ is obtained for the solid line when points a, d, and h are excluded from the regression procedure. The R value for the dashed line, where all the points are used in the regression, is 0.776.

outlyers, showing the largest deviations from the "best-fit" straight line through the reported points. Indeed the value of the coefficient of correlation is $R = 0.776$ for the 12 points reported in the plot, while the coefficient increases to $R = 0.931$ when points a, d, and h are excluded from the regression procedure.

The Mo–O distance (1.955 Å) in the chain along the *c* axis (Table III) is very close to the critical overlap distance (smaller values allow Mo (d_{t2g}) –O $(p\pi)$ overlap) found (*12*, *13*) for the K blue bronze, thus indicating that, through this route, only small conduction, if any, is possible. In the *ab* plane no conduction is possible, based on Mo–O bonds, since in that plane one can see only sequences of short and very long (>2.2 Å) distances. The shortest Mo–Mo distance (3.324 Å, through the edge shared by two adjacent coordination "octahedra") is too large for any significant metal–metal interaction. In conclusion, only a small one-dimensional conduction in the Mo–O–Mo–O– chain along the *c* axis seems possible in the title compound on the basis of its structure.

Conclusions

It is well known that metallic conduction in these materials can be attributed to the presence of electrons in the π^* antibonding orbitals (*1*) and therefore the correlation between ξ and v can be extended to the conduction properties. Indeed the smallest distortions are shown by γ-Mo_4O_{11}, a well-known bidimensional metallic conductor (*11*), while the blue bronzes are known to be quasi-one-dimensional conductors showing a transition to a semiconductor state (*12*, *13*). In the latter materials most of the Mo 4*d* electrons are located in two Mo sites, those corresponding to points l and m in Fig. 4, while only a small portion of those electrons are located at the third crystallographically independent Mo site, corresponding to the highly distorted "octahedron" represented by point i. Point n, corresponding to the Mo coordination "octahedron" of the title compound, is even more distorted and characterized by a higher value of v.

Acknowledgments

The authors acknowledge financial support by the "Progetto Finalizzato Materiali Speciali per Tecnologie Avanzate," CNR, Rome, Italy, and thank A. Albinati for useful discussions while the diffraction experiment was being planned and T. Pilati for kindly allowing us to use the POLIEDRI program.

References

1. M. Greenblatt, *Chem. Rev.* **88,** 31 (1988).
2. P. P. Tsai, J. A. Potenza, and M. Greenblatt, *J. Solid State Chem.* **69,** 329 (1987).
3. S. C. Abrahams, P. Marsh, L. F. Schneemeger, C. E. Rice, and S. E. Spengler, *J. Mater. Res.* **2,** 82 (1987).
4. M. Zocchi, L. E. Depero, and F. Zocchi, *J. Solid State Chem.* **92,** 18 (1991).
5. F. Zocchi, Italian Patent No. 1198264, Dec. 21, 1988; application filed on Dec. 24, 1986.
6. A. C. North, D. C. Phillips, and F. S. Mathews, *Acta Crystallogr. Sect. A* **24,** 351 (1968).
7. "International Tables for X-ray Crystallography," Vol IV, Kynoch, Birmingham (1974).
8. B. A. Frenz and Associates, "SDP plus Version 1.0," Enraf–Nonius, Delft (1980).
9. B. M. Gatehouse and B. K. Minskin, *Acta Crystallogr. Sect. B* **31,** 1293 (1975).
10. I. D. Brown and K. K. Wu, *Acta Crystallogr. Sect. B* **32,** 1957 (1976).
11. M. Ghedira, H. Vincent, M. Marezio, J. Marcus, and G. Furcaudot, *J. Solid State Chem.* **56,** 66 (1985).
12. G. Travaglini and P. Wachter, *Solid State Commun.* **47,** 217 (1983).
13. W. Shutte, "Structures of Modulated Crystals," Ph.D. Thesis, University of Groningen (1990).